Histol Histopathol (2023) 38: 1179-1192

Histology and Histopathology
From Cell Biology to Tissue Engineering

ORIGINAL ARTICLE Open Access

Matrine inhibits hepatocellular carcinoma cell malignancy through the circ_0013290/miR-139-5p/MMP16 pathway

Xinfeng Chang[1]*, Zhengchun Huang[2]*, Zhihua Zhang[3], Wen Pan[4] and Chunhua Song[5]

[1]Department of Human Anatomy, Jiangsu Vocational College of Medicine, [2]Department of Human Anatomy, Gannan Medical University, [3]Department of Graduate, Gannan Medical University, [4]Department of Physiology, Jiangsu Vocational College of Medicine and [5]Department of Surgery, Jiangsu Vocational College of Medicine, Jiangsu Province, China

*These authors contributed equally to this work

Summary. Background. Previous studies have shown the anticancer effect of Matrine on hepatocellular carcinoma (HCC); however, the underlying mechanism is still indistinct.

Methods. The expression of circular RNA_0013290 (circ_0013290), microRNA-139-5p (miR-139-5p), matrix metallopeptidase 16 (MMP16), CyclinD1 and N-cadherin was analyzed by quantitative real-time polymerase chain reaction, Western blotting or immunohistochemistry assay. Cell viability, proliferation, apoptosis, invasion and tube formation were analyzed by cell counting kit-8, 5-Ethynyl-2'-deoxyuridine, flow cytometry analysis, transwell invasion and tube formation assays, respectively. The associations among circ_0013290, miR-139-5p and MMP16 were predicted by starbase online database, and identified by dual-luciferase reporter and RNA pull-down assays. A xenograft mouse model assay was conducted to disclose the effects of circ_0013290 and Matrine on tumor tumorigenesis *in vivo*.

Results. Circ_0013290 and MMP16 expression were significantly upregulated, while miR-139-5p was downregulated in HCC tissues and cells compared with the matched normal liver tissues and cells. Matrine treatment inhibited HCC cell proliferation, invasion and tube formation but induced cell apoptosis, accompanied by the decrease of CyclinD1 and N-cadherin expression; however, these effects were counteracted when circ_0013290 expression was increased. MiR-139-5p depletion or MMP16 introduction relieved Matrine-induced effects in HCC cells. The regulation of circ_0013290 toward HCC cell processes involved MMP16. With respect to the mechanism, circ_0013290 acted as a miR-139-5p sponge, and miR-139-5p targeted MMP16 in HCC cells. Besides, circ_0013290 regulated MMP16 expression through miR-139-5p. Further, circ_0013290 depletion enhanced the inhibitory effects of Matrine on tumor tumorigenesis.

Conclusion. Matrine inhibited HCC cell malignancy through the circ_0013290/miR-139-5p/MMP16 pathway, suggesting that Matrine is a potential therapeutic agent for HCC.

Key words: HCC, Matrine, circ_0013290, miR-139-5p, MMP16

Corresponding Author: Chunhua Song, Hengda Mingdu Garden Community, 170 Shenzhou Road, Yandu District, Yancheng City, Jiangsu Province, 224005, China. e-mail: songchunhua81@163.com
www.hh.um.es. DOI: 10.14670/HH-18-574

Introduction

Hepatocellular carcinoma (HCC) is derived from liver parenchymal cells, hepatocytes, and is the fourth leading cause of tumor-related deaths globally with a dismal 5-year survival rate of about 18%, accounting for around 80% of all liver tumors (Draper, 2020; Sung et al., 2021). HCC commonly develops in the presence of hepatitis virus (type B or C), or alcoholic cirrhosis (Intaraprasong et al., 2016). In addition, aflatoxin exposure, glycogen storage disease, obesity, diabetes and biliary cirrhosis increase the susceptibility to this cancer (Paganoni et al., 2021). Despite substantial progress in therapy, HCC patients still have poor prognoses because of tumor metastasis and recurrence (Sohal and Sun, 2011). Thus, investigating the mechanism of HCC development and exploring effective therapeutic methods for HCC are necessary to improve the unfavorable prognosis.

Natural products have widespread biological activities, and have been sources of anticancer agents. Matrine ($C_{15}H_{24}N_2O$) is a quinolizidine alkaloid compound that is isolated from some herbs, such as *Sophora flavescens* and *Sophora alopecuroides* (Zhu et

al., 2016). As reported, the bio-active agent has different effects on cell apoptosis, cancer progression, fibrotic tissue development and inflammatory response (Zhang et al., 2019). It has been demonstrated that Matrine has anti-malignant activities against prostate cancer (PC) (Huang et al., 2018), pancreatic cancer (Cho et al., 2018), and glioblastoma (Zhou et al., 2018). Moreover, State Food and Drug Administration has supported the use of Matrine in anticancer treatment (Rashid et al., 2019). However, whether Matrine has anticancer effects against HCC still needs further investigation.

Circular RNA (circRNA) is a protein-coding or non-coding RNA and has been attracting much attention recently. Circular RNA is generated from head-to-tail splicing of precursor mRNA, and is abundantly expressed in human cells (Qu et al., 2015). The functional effects of circRNA on HCC development have been widely studied (Zhang et al., 2020b). In addition, circRNA participated in the regulation of Matrine toward cancer development. For example, Matrine inhibited circ_0027345 to suppress HCC cell growth, motility and induce autophagy (Lin et al., 2020). Chi et al. reported that Matrine increased glioma cell apoptosis and autophagy by regulating circ_104075 (Chi et al., 2019). In particular, circ_0013290 has been explained to be a cancer-promoting gene in HCC (Luo et al., 2021); however, whether Matrine combines with circ_0013290 to inhibit HCC cell malignancy remains unclear.

Increasing evidence shows that circRNA functions by sponging microRNA (miRNA) (Kulcheski et al., 2016; Panda, 2018). Consisting of 18-25 nucleotides, miRNA is a noncoding transcript that promotes or inhibits tumor progression through posttranscriptional regulation toward oncogene or tumor-suppressor genes (Hua et al., 2018). The underlying mechanism of Matrine regulating cancer development involves miRNAs (Wei et al., 2018). MiR-139-5p, a small miRNA, regulates the progression of colorectal cancer (Du et al. 2020a), lung adenocarcinoma (Li et al. 2020) and HCC (Wu et al. 2020). However, whether and how miR-139-5p is associated with the inner mechanism of Matrine modulating HCC progression still needs further investigation.

Through the prediction of starbase database ((http://starbase.sysu.edu.cn/agoClipRNA.php?source=mRNA), we found that circ_0013290 potentially bound to miR-139-5p. On that account, we hypothesized that the circ_0013290/miR-129-5p pathway participated in the regulation of Matrine toward HCC development. Thus, the work analyzed the functional effects of Matrine on HCC cell motility, apoptosis, tube formation and growth, and determined whether the underlying mechanism involved circ_0013290 and miR-139-5p. Besides, we identified the downstream gene of the circ_0013290/miR-139-5p axis based on the competing endogenous RNA theory that indicated circRNA could serve as a miRNA sponge to inhibit mRNA degradation by miRNA-associated pathways (Salmena et al., 2011).

Materials and methods

Clinical HCC specimens

HCC tissues and adjacent healthy liver tissues were harvested from 26 patients with HCC during surgery in Jiangsu Vocational College of Medicine with the approval from Jiangsu Vocational College of Medicine. The 26 pairs of tissues were stored at -80°C for future assays. Each participant signed written informed consent before the surgery.

Cell culture and treatment

HCC cell lines (Hep3B and Huh-7) were provided by Sunncell Biotech (Wuhan, China), and maintained in DMEM (Sunncell Biotech). Human immortal liver cells (THLE-2) and human umbilical vein endothelial cells (HUVECs) were purchased from X-Y Biothech (Shanghai, China) and cultured in RPMI-1640 (Sunncell Biotech) or DMEM. The corresponding medium was added with 10% fetal bovine serum (FBS) and 1% penicillin/streptomycin. Routine culture was performed at 37°Cin a biochemical incubator (Hanuo, Shanghai, China) buffered with 5% CO_2.

Hep3B and Huh-7 cells were stimulated by various concentrations of Matrine (0, 0.5, 1 or 1.5 mg/mL; Yuanye Biotech, Shanghai, China) for 48 h to analyze the functional effects of Matrine on HCC cell processes.

Plasmid construction

Hep3B and Huh-7 cells were allowed to grow in 12-well plates and cell transfection was performed the next day following the guidebook of LipoFiter (Hanbio, Shanghai, China). After cell transfection for 6h, the medium was removed and a complete medium containing 10% fetal bovine serum was added into each well. After 48h, transfection efficiency was analyzed for functional assays. Circ_0013290 and MMP16 overexpression plasmids were generated by GENEWIZ (Suzhou, China) using the full-length circ_0013290, the coding sequence of MMP16, pCD5-ciR vector and pcDNA 3.1 (+) vector. The mimics of miR-139-5p (miR-139-5p, 5'-UCUACAGUGCACGUGUCUCCAGU-3'), the inhibitors of miR-139-5p (anti-miR-139-5p, 5'-ACUGGAGACACGUGCACUGUAGA-3'), the small hairpin RNA of circ_0013290 (sh-circ_0013290, 5'-AGCTGAGCTGCTAATAGTAAA-3') and the matched controls (miR-NC, anti-miR-NC and sh-NC) were synthesized by GenePharma (Shanghai, China).

Cell viability analysis

Hep3B and Huh-7 cells were allowed to grow in 96-well plates for 12h, and then treated with various concentrations of Matrine (0, 0.5, 1 or 1.5 mg/mL; Yuanye Biotech) or transfected with circ_0013290

overexpression plasmid, pCD5-ciR, anti-miR-139-5p, anti-miR-NC, MMP16-overexpressing plasmid, pcDNA, sh-circ_0013290 and sh-NC. At the defined time, the cells were exposed to cell counting kit-8 (CCK-8) reagent (KeyGen, Nanjing, China), and incubated in cell culture incubators for 3h. Finally, the data measured on a microplate reader (REAGEN, Shenzhen, China) were recorded.

Cell proliferation

5-Ethynyl-2'-deoxyuridine (EdU) Imaging Kit (APExBIO Technology, Shanghai, China) was used to analyze the proliferative ability of Hep3B and Huh-7 cells with various treatments. In brief, the Hep3B and Huh-7 cells were incubated with EdU in a cell culture incubator for 2h, fixed with paraformaldehyde for 15 min and penetrated with 0.5% Triton®X-100 for 20 min at room temperature. Then, the click reaction was conducted according to the guidebook. The cells were stained using 4',6-Diamidino-2-Phenylindole (DAPI) and analyzed by fluorescence microscope (Olympus, Tokyo, Japan).

Flow cytometry analysis

In accordance with the producer's guidance, HCC cell apoptosis was assessed using an Annexin V-FITC apoptosis detection kit (BioVision, Milpitas, California, USA). Transfected Hep3B and Huh-7 cells were harvested and suspended in Binding Buffer, followed by incubating with Annexin V-FITC and propidium iodide for 10 min in a dark place. Finally, cell apoptosis was monitored utilizing a flow cytometer (Luminex, Shanghai, China).

Cell invasion assay

Transwell chambers pre-coated with Matrigel (Qcbio science, Shanghai, China) were used to analyze the invasive ability of Hep3B and Huh-7 cells as instructed (Xu et al., 2020). After various treatments, the cells were re-suspended in serum-free DMEM (Sunncell Biotech) and added into the upper chambers, while the complete DMEM containing 15% FBS (Sunncell Biotech) was placed into the lower chambers. After 24h of culture, paraformaldehyde was used to fix the cells invading through the Matrigel. The cells were stained by crystal violet, and photographed under an inverted microscope (Luminex).

Tube formation assay

According to the previous method (He et al., 2019), Matrigel assay was conducted to analyze *in vitro* angiogenesis ability of HCC cells. In total, HUVECs were first cultured in 6-well plates and subjected to various treatments. After 48h, the cells were passaged in 96-well plates, pre-coated with growth factor-depleted Matrigel (Qcbio science), supplemented with HCC cells-conditioned medium, and cultured for 12h. The picture of each well was taken using microscopy (Olympus). Cell angiogenic capacity was evaluated by counting branches using Image J software.

Western Blotting assay

NP-40 lysis buffer plus proteinase inhibitor (Yeasen, Shanghai, China) was used to extract total proteins from HCC patients, cells and primary tumors from Huh-7 cells. 20 μg of proteins, as quantified by BCA protein assay, was separated by SurePAGE gels (Thermo Fisher, Waltham, MA, USA), and then transferred onto polyvinylidene difluoride membranes. Skimmed dry milk was used to block the non-specific binding on the membranes. The membranes were probed with the following antibodies: anti-CyclinD1 (#AHF0082; 1:1000; Thermo Fisher), anti-N-cadherin (#33-3900; 1:1000; Thermo Fisher), MMP16 (#PA5-79680; 1:1000; Thermo Fisher), and glyceraldehyde 3-phosphate dehydrogenase (GAPDH) (#437000; 1:500; Thermo Fisher). After being incubated with secondary antibodies, the membranes were analyzed using ECL Detection System (Thermo Fisher).

Quantitative real-time polymerase chain reaction (qRT-PCR)

Based on the manufacturer of TsingZol (Tsingke, Shanghai, China), we isolated total RNA from tissues and cells. Goldenstar™ RT6 cDNA Synthesis reagents (Tsingke) as well as miRNA synthesis kit (Thermo Fisher) were used for reverse transcription. Meanwhile, RNase R (Xiyuan Biotechnology, Shanghai, China) was utilized for the determination of circular circ_0013290 in HCC cells as instructed (Xu et al., 2020). To quantify gene expression, SYBR Mix (Thermo Fisher) was mixed with cDNA and primers (shown in Table 1), and then reacted on a 96-well thermocycler (Bio-Rad, Hercules, CA, USA). Gene expression was analyzed by the $2^{-\Delta\Delta Ct}$ method with the normalization to U6 or GAPDH.

Table 1. Primer sequences used in qRT-PCR.

Name	Primers for qRT-PCR (5'-3')	
hsa_circ_0013290	Forward	CTGAGCTGCTAATAGTAAATGG
	Reverse	ACGCCAAAGTGCTCTGTCTAA
MMP16	Forward	ACAGGAACTACTGCTGACCCT
	Reverse	TGCACGAAATCCAACCGTCT
miR-139-5p	Forward	GTATGAGTCTACAGTGCACGTGTC
	Reverse	CTCAACTGGTGTCGTGGAG
GAPDH	Forward	AGCTCACTGGCATGGCCTTC
	Reverse	CGCCTGCTTCACCACCTTCT
U6	Forward	CTTCGGCAGCACATATACT
	Reverse	AAAATATGGAACGCTTCACG

Dual-luciferase reporter assay

The binding sites of circ_0013290 and MMP16 with miR-139-5p were predicted by starbase online database (http://starbase.sysu.edu.cn/agoClipRNA.php?source=mRNA). The sequences of circ_0013290 and MMP16 containing the complementary sites were amplified by PCR and then inserted into the pmirGLO vector to generate wild-type plasmids, including WT-circ_0013290 and WT-MMP16 3'UTR. Site-directed mutant circ_0013290 and MMP16 were generated using a Site-Directed Mutagenesis Kit (Yeasen) to build mutant reporter plasmids, including MUT-circ_0013290 and MUT-MMP16 3'UTR. Then, the reporter plasmids were co-transfected into Hep3B and Huh-7 cells with miR-139-5p mimics or miR-NC using LipoFiter (Hanbio). Employing a Dual-Lucy Assay Kit (Solarbio, Beijing, China), we analyzed luciferase activity in the transfected cells after 48h as per the guidebook.

RNA pull-down assay

GenePharma Co., Ltd. provided biotinylated miR-139-5p (bio-miR-139-5p) and biotinylated miR-NC (bio-miR-NC). Hep3B and Huh-7 cells were transfected with 50 nM biotin, and RIP lysis buffer was used to lyse the cells for 10 min. Then, cell supernatants were collected and incubated with streptavidin-coupled beads (Sigma-Aldrich, St. Louis, MO, USA). The combined RNAs in the complexes were purified, and circ_0013290 and MMP16 enrichment were analyzed by qRT-PCR.

Tumor formation in vivo

Twenty-four male BALB/C nude mice (age, 4 weeks; weight, 17-20 g) were provided by Charles River (Beijing, China), and raised in pathogen-free cabinets. These mice were averagely grouped into 4 groups. 5×10^6 Huh-7 cells transfected with sh-circ_0013290 or sh-NC were injected into the mice subcutaneously. When forming tumors were visible, the mice were administrated with Matrine (45 mg/kg; Yuanye Biotech) every 3 days for 5 cycles. Meanwhile, tumor volume was recorded every 3 days according to volume=0.5 × width^2 × length. After 23 days of injection, the neoplasms were harvested for analysis of tumor weight

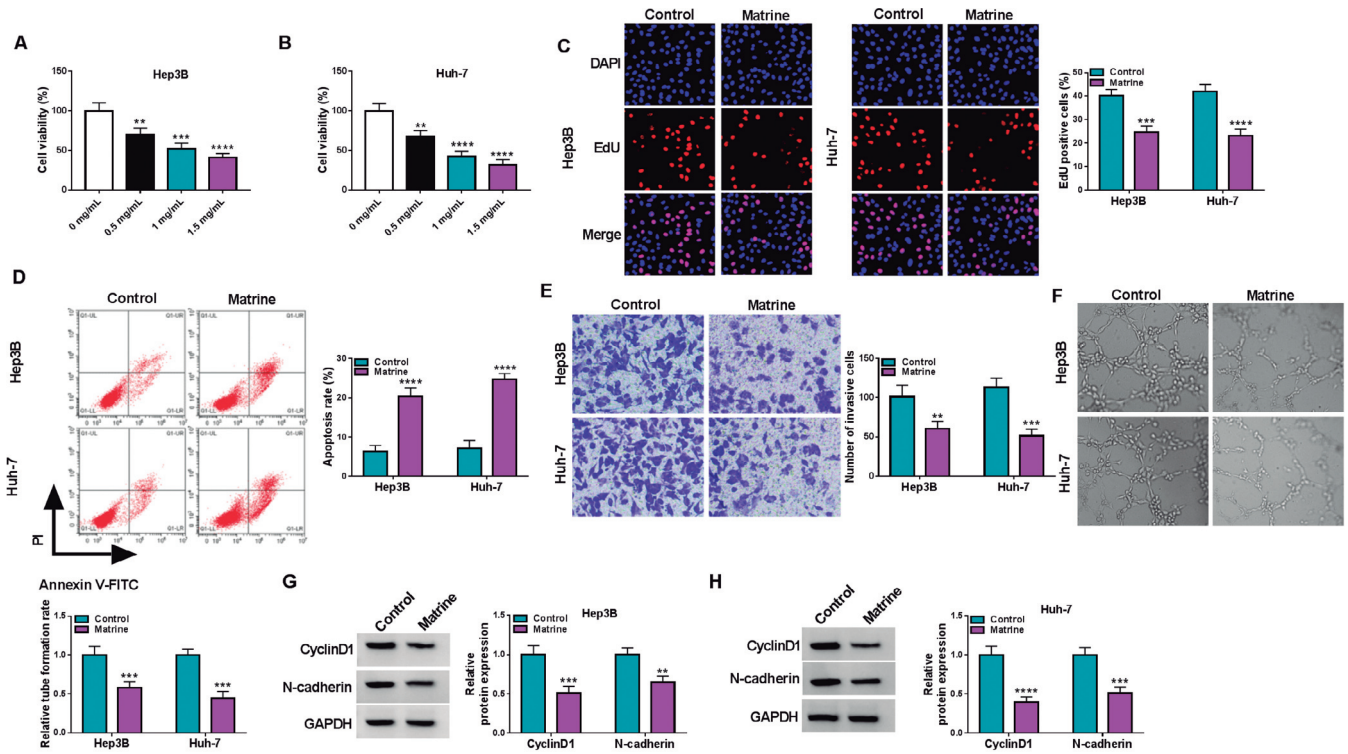

Fig. 1. Matrine inhibited HCC cell malignancy. **A, B.** The effects of various concentrations of Matrine (0, 0.5, 1 or 1.5 mg/mL) on Hep3B and Huh-7 cell viability were analyzed by CCK-8 assay. **C.** EdU assay was performed to determine 1 mg/mL Matrine-induced effects on the proliferation of Hep3B and Huh-7 cells. **D.** Flow cytometry analysis was carried out to investigate the effect of 1 mg/mL Matrine treatment on Hep3B and Huh-7 cell apoptosis. **E.** Transwell invasion assay was used to evaluate the impact of Matrine treatment (1 mg/mL) on Hep3B and Huh-7 cell invasion. **F.** Tube formation assay was conducted to determine the effect of Matrine treatment (1 mg/mL) on the angiogenesis of Hep3B and Huh-7 cells. **G, H.** The protein expression of CyclinD1 and N-cadherin was detected by Western blotting analysis in the Hep3B and Huh-7 cells treated with or without Matrine (1 mg/mL). ***P*<0.01, ****P*<0.001 and *****P*<0.0001.

and gene expression. In addition, we reveived approval from the Animal Care and Use Committee of Jiangsu Vocational College of Medicine before conducting the experiment.

Immunohistochemistry staining

Xenograft tumors were employed for further analysis of MMP16, CyclinD1 and N-cadherin expression *in vivo* as instructed (Huang et al., 2017). Sections were embedded in paraffin, and then immersed in sodium citrate for 20 min to repair antigen. After that, the sections were incubated with anti-MMP16 (#PA5-79680; 1:100; Thermo Fisher), anti-CyclinD1 (#PA5-32373; 1:200; Thermo Fisher) and N-cadherin (PA5-29570; 1:200; Thermo Fisher) for a whole night. The sections were probed with secondary antibodies. Finally, a microscope (Olympus) was applied to analyze the samples.

Statistical processing

GraphPad Prism software was used to analyze the data from 3 independent duplicate tests, and results are shown as means ± standard deviations (SD). We utilized Spearman's correlation test to analyze the association between two groups. The statistical differences in other groups were compared with two-tailed Student's *t*-tests,

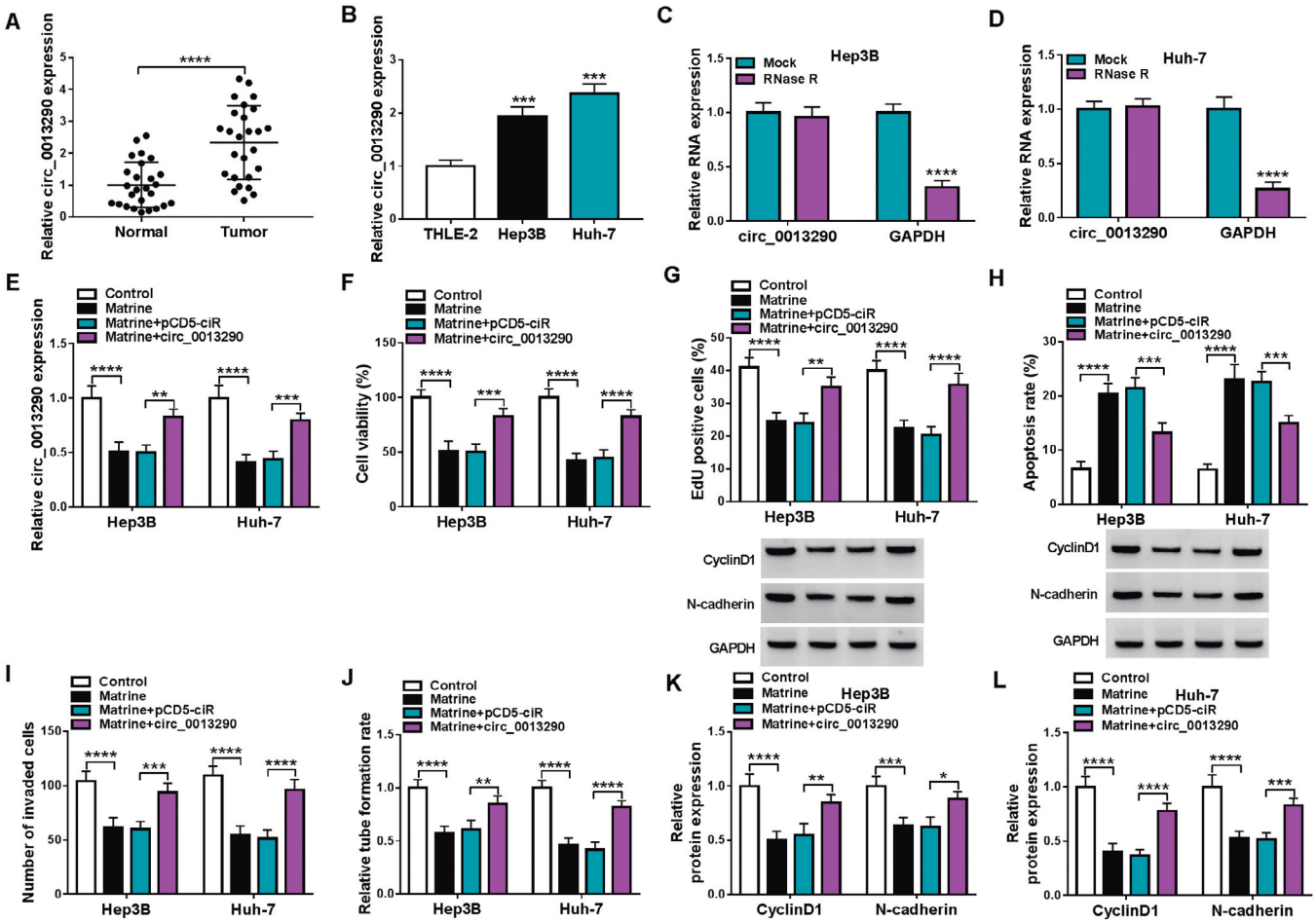

Fig. 2. Circ_0013290 overexpression counteracted the effects of Matrine on HCC cell processes. **A, B.** Circ_0013290 expression was analyzed by qRT-PCR in HCC tissues (N=26), the matched normal liver tissues (N=26), THLE-2 cells, Hep3B cells and Huh-7 cells. **C, D.** The circular structure of circ_0013290 was identified by RNase R treatment assay. **E-L.** Hep3B and Huh-7 cells were divided into control (untreated cells), Matrine, Matrine+pCD5-ciR and Matrine+circ_0013290 groups, and circ_0013290 expression was analyzed by qRT-PCR **(E)**, cell viability by CCK-8 assay **(F)**, cell proliferation by EdU assay **(G)**, cell apoptosis by flow cytometry analysis **(H)**, cell invasion by transwell invasion assay **(I)**, cell angiogenic capacity by tube formation assay **(J)**, and the protein expression of CyclinD1 and N-cadherin by Western blotting analysis **(K, L)**. **P*<0.05, ***P*<0.01, ****P*<0.001 and *****P*<0.0001.

Wilcoxon signed-rank test, one-way analysis of variance or Kruskal-Wallis test. $P<0.05$ indicated a statistical significance.

Results

Matrine inhibited HCC cell proliferation, invasion and tube formation but induced apoptosis

The study first analyzed the effects of Matrine (0, 0.5, 1 or 1.5 mg/mL) on HCC cell processes, including cell proliferation, apoptosis, invasion and angiogenesis. As shown in Fig. 1A,B, Matrine treatment concentration-dependently inhibited the viability of Hep3B and Huh-7 cells. 1 mg/mL Matrine was used in the following study. Comparatively, Matrine stimulation inhibited proliferation but induced apoptosis of Hep3B and Huh-7 cells (Fig. 1C,D). In addition, the invasion and tube formation of Hep3B and Huh-7 cells were suppressed after Matrine treatment (Fig. 1E,F). Further, we assessed the expression of proliferation-related CyclinD1 and metastasis-associated N-cadherin by Western blotting analysis in Matrine-induced Hep3B and Huh-7 cells. As expected, we observed a lower expression of the two proteins in the cells compared with the untreated cells (Fig. 1G,H).

Circ_0013290 overexpression counteracted the effects of Matrine on HCC cell processes

Then, circ_0013290 expression in HCC tissues and cells was examined by qRT-PCR. As presented in Fig. 2A, circ_0013290 expression was significantly upregulated in the HCC tissues compared with the adjacent healthy tissues (>3 cm away from the cancerous tissues). Meanwhile, we observed a higher expression of circ_0013290 in HCC cell lines (Hep3B and Huh-7) than in normal liver cell line (THLE-2) (Fig. 2B). The RNase R treatment assay indicated the circular structure of circ_0013290 (Fig. 2C,D). Subsequently, we overexpressed circ_0013290 in Matrine-treated Hep3B and Huh-7 cells to explore the consequent effects on Matrine-mediated cell processes. Fig. 2E shows that Matrine treatment reduced circ_0013290 expression, whereas the effect was relieved after circ_0013290 overexpression. The inhibitory effects of Matrine on cell viability and proliferation were rescued when circ_0013290 expression was increased (Fig. 2F,G). In addition, the increased cell apoptosis and decreased cell invasive ability by Matrine were remitted after circ_0013290 introduction (Fig. 2H,I). Matrine stimulation inhibited the angiogenic capacity of Hep3B and Huh-7 cells, but the effect was restored by

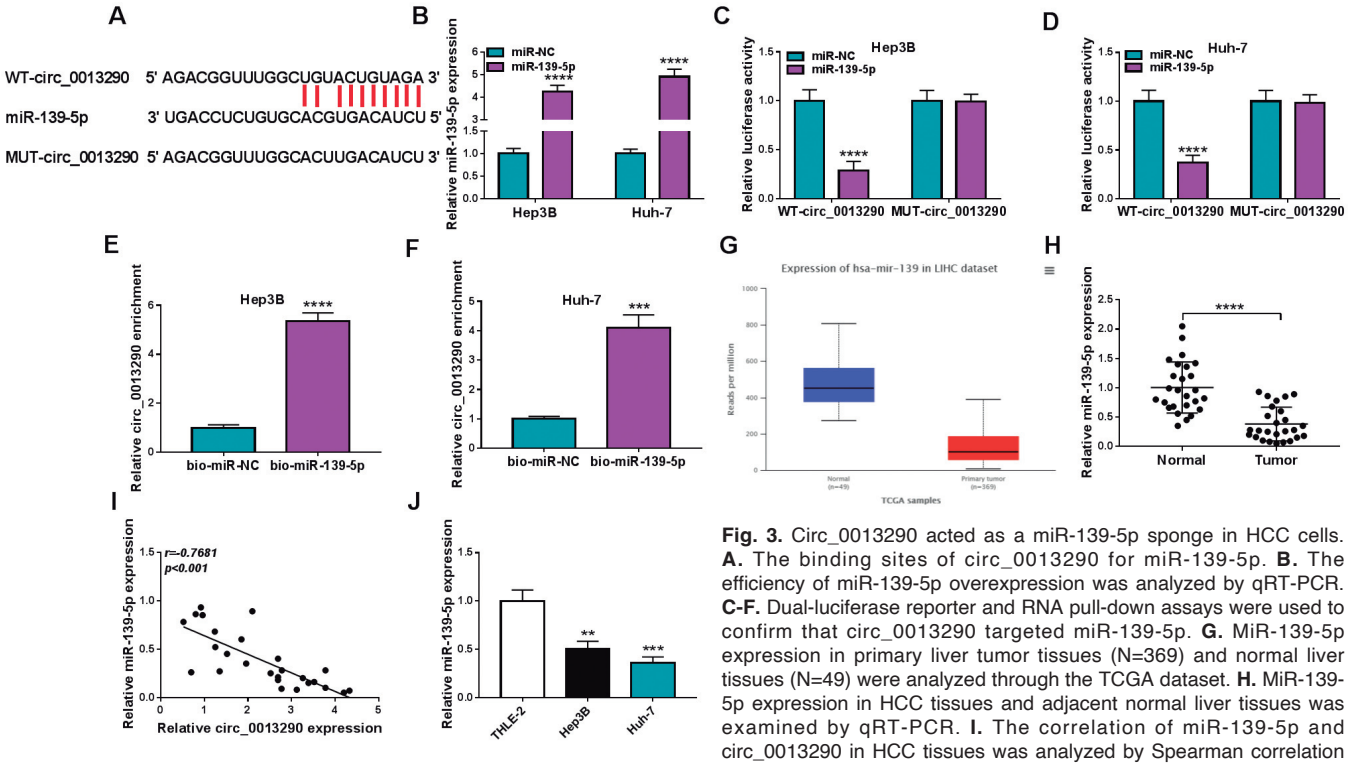

Fig. 3. Circ_0013290 acted as a miR-139-5p sponge in HCC cells. **A.** The binding sites of circ_0013290 for miR-139-5p. **B.** The efficiency of miR-139-5p overexpression was analyzed by qRT-PCR. **C-F.** Dual-luciferase reporter and RNA pull-down assays were used to confirm that circ_0013290 targeted miR-139-5p. **G.** MiR-139-5p expression in primary liver tumor tissues (N=369) and normal liver tissues (N=49) were analyzed through the TCGA dataset. **H.** MiR-139-5p expression in HCC tissues and adjacent normal liver tissues was examined by qRT-PCR. **I.** The correlation of miR-139-5p and circ_0013290 in HCC tissues was analyzed by Spearman correlation analysis. **J.** MiR-139-5p expression was detected by qRT-PCR in THLE-2, Hep3B and Huh-7 cells. LIHC: liver hepatocellular carcinoma; TCGA: The Cancer Genome Atlas. **$P<0.01$, ***$P<0.001$ and ****$P<0.0001$.

increasing circ_0013290 expression (Fig. 2J). Further, the inhibitory effects of Matrine treatment on the protein expression of CyclinD1 and N-cadherin were attenuated after circ_0013290 introduction (Fig. 2K,L). These results suggested that circ_0013290 participated in the regulation of Matrine toward HCC cell processes.

Circ_0013290 acted as a miR-139-5p sponge in HCC cells

Starbase online database was employed to predict the target miRNAs of circ_0013290. As shown in Figure 3A, miR-139-5p carried the binding sites of circ_0013290, indicating the potential regulatory relationship of circ_0013290 and miR-139-5p. Subsequently, dual-luciferase reporter and RNA pull-down assays were conducted to analyze whether miR-139-5p was a target miRNA of circ_0013290. Before that, we confirmed the success of miR-139-5p overexpression using qRT-PCR (Fig. 3B). As presented in Figure 3C,D, miR-139-5p mimics significantly inhibited the luciferase activity of wild-type reporter plasmid of circ_0013290, but not that of mutant reporter plasmid. Meanwhile, we observed that biotinylated miR-139-5p dramatically enriched circ_0013290 compared with the biotinylated miR-NC group (Fig. 3E,F). The above data indicated that circ_0013290 bound to miR-139-5p. Consistently, miR-139-5p expression was analyzed through the TCGA dataset. As shown in Figure 3G, miR-139-5p expression was lower in primary liver tumor tissues than in normal liver tissues. Comparatively, miR-139-5p expression was significantly downregulated, and negatively correlated with circ_0013290 expression in HCC tissues (Fig. 3H,I). The lower expression of circ_0013290 was also observed in HCC cells (Hep3B and Huh-7) compared with the normal liver cells (THLE-2) (Fig. 3J).

MiR-139-5p inhibitors attenuated Matrine-induced effects in Hep3B and Huh-7 cells

Given the regulatory relationship of circ_0013290 and miR-139-5p, we continued to analyze whether miR-139-5p participated in the regulation of Matrine toward Hep3B and Huh-7 cell processes. To explain this, we silenced miR-139-5p expression in Matrine-stimulated Hep3B and Huh-7 cells. As shown in Figure 4A, Matrine treatment increased miR-139-5p expression, while the effect was relieved after miR-139-5p depletion. Subsequently, Matrine inhibited cell viability and cell proliferation, whereas these effects were restored when miR-139-5p expression was reduced (Fig. 4B,C). The promoting effect of Matrine on cell apoptosis and the inhibitory effects on cell invasion and tube

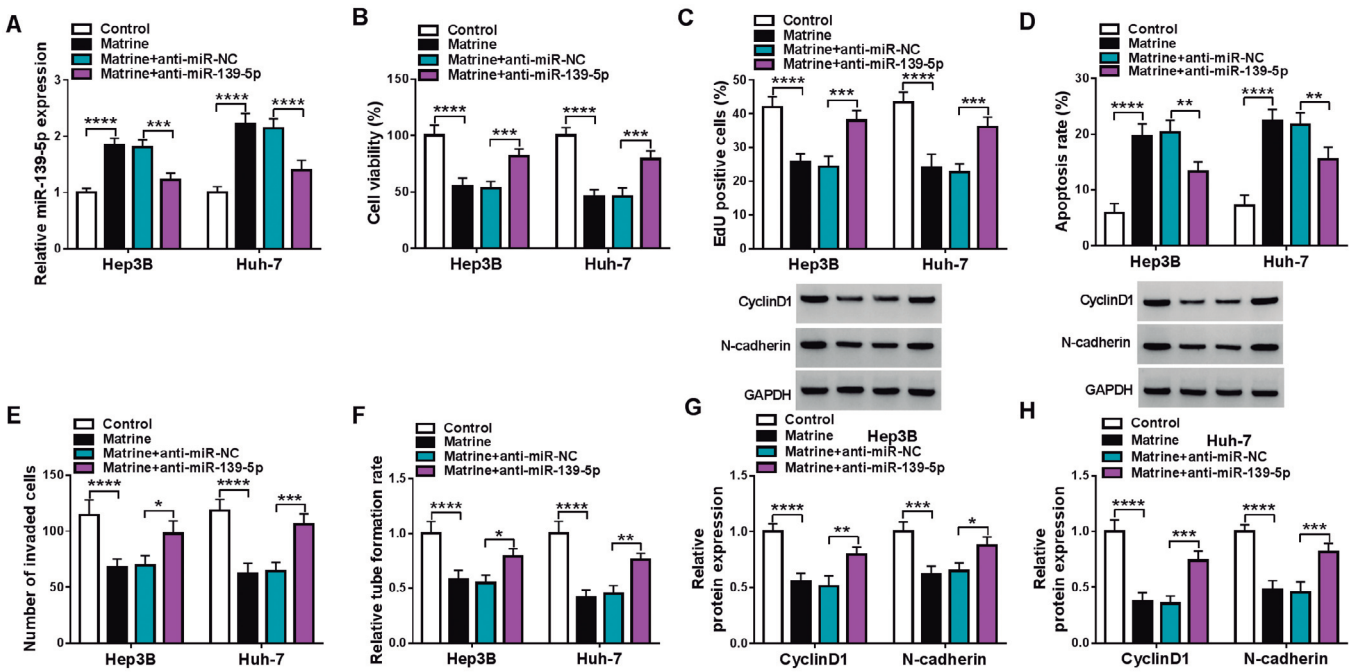

Fig. 4. Matrine inhibited HCC cell processes by regulating miR-139-5p. Hep3B and Huh-7 cells were treated with Matrine, Matrine+anti-miR-NC or Matrine+anti-miR-139-5p. Untreated Hep3B and Huh-7 cells were used as controls. **A.** MiR-139-5p expression was detected by qRT-PCR. **B.** Cell viability was analyzed by CCK-8 assay. **C.** Cell proliferation was evaluated by EdU assay. **D.** Flow cytometry analysis was performed to assess cell apoptosis. **E.** Transwell invasion assay was conducted to analyze cell invasion. **F.** The tube formation of Hep3B and Huh-7 cells was investigated by tube formation assay. **G, H.** The protein expression of CyclinD1 and N-cadherin was checked by Western blotting analysis. **P*<0.05, ***P*<0.01, ****P*<0.001 and *****P*<0.0001.

formation were rescued after miR-139-5p knockdown (Fig. 4D-F). Further, decreasing miR-139-5p expression attenuated the inhibitory effects of Matrine on the protein expression of CyclinD1 and N-cadherin (Fig. 4G,H). These findings demonstrated that Matrine inhibited HCC cell processes by regulating miR-139-5p.

MiR-139-5p targeted MMP16 in HCC cells

The target gene of miR-139-5p was further predicted by starbase online database. Figure 5A shows that MMP16 contained the complementary sites of miR-139-5p, suggesting that MMP16 might be a target gene of miR-139-5p. Then, the potential regulatory relationship of miR-139-5p and MMP16 was elucidated by dual-luciferase reporter and RNA pull-down assays. We observed that miR-139-5p overexpression reduced the luciferase activity of wild-type reporter plasmid of MMP16 rather than that of mutant reporter plasmid of MMP16 (Fig. 5B,C). Moreover, we found that MMP16 was significantly enriched in the bio-miR-139-5p group compared with its expression in the bio-miR-NC group (Fig. 5D,E). Consistently, MMP16 expression was dramatically increased, and was negatively correlated with miR-139-5p expression in HCC tissues (Fig. 5F-H). Further, it was found that MMP16 expression was higher in HCC cells (Hep3B and Huh-7 cells) than in normal liver cells (THLE-2) (Fig. 5I). The above results demonstrated that miR-139-5p targeted MMP16.

Matrine suppressed HCC cell malignancy by modulating MMP16

MMP16 overexpression plasmid was transfected into Matrine-induced Hep3B and Huh-7 cells to investigate the consequent effects on cell processes. As presented in Figure 6A, Matrine reduced MMP16 expression in the cells, whereas the effect was remitted

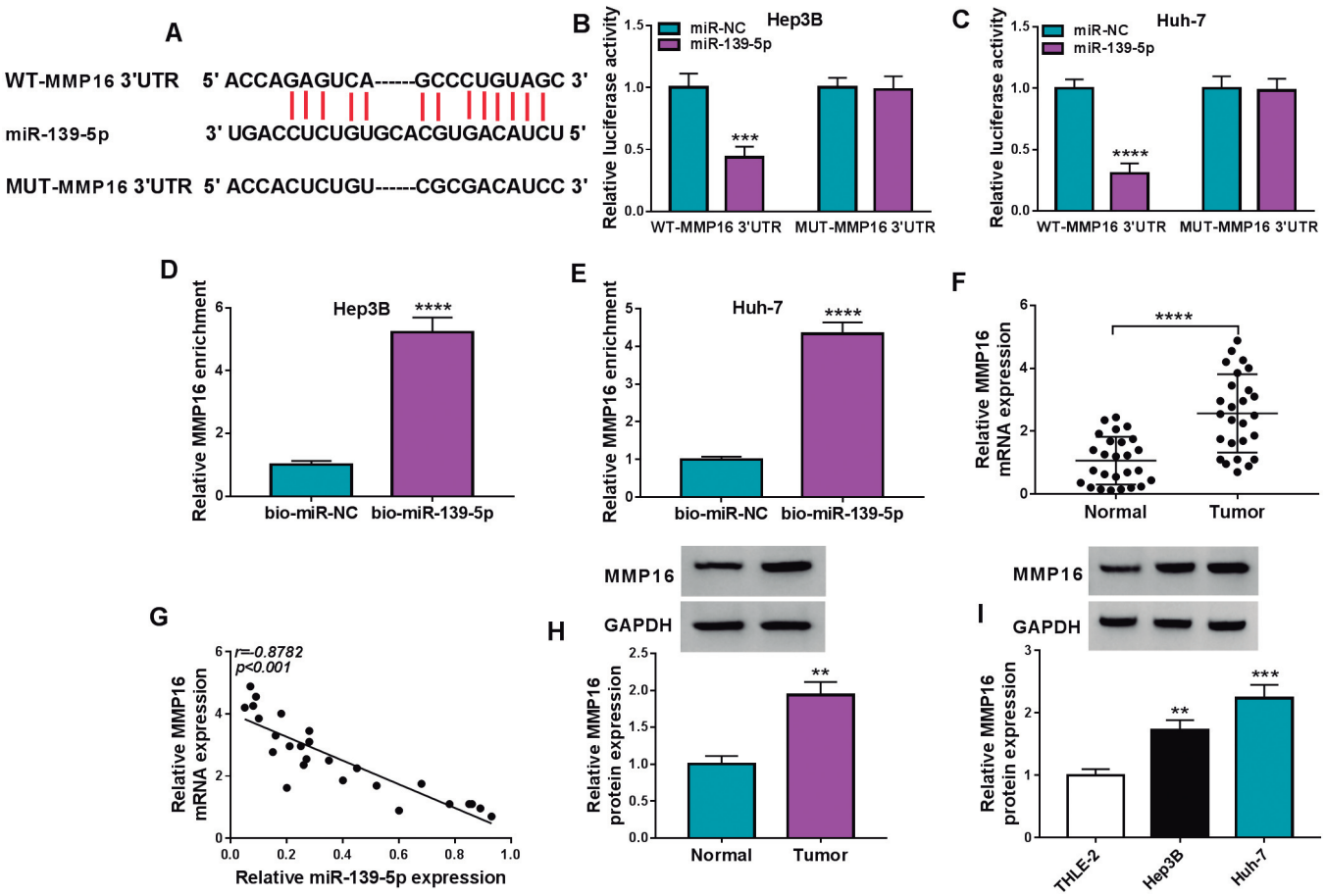

Fig. 5. MiR-139-5p was associated with MMP16 in HCC cells. **A.** The binding sites of miR-139-5p for MMP16. **B-E.** The association of miR-139-5p with MMP16 was identified by dual-luciferase reporter and RNA pull-down assay. **F, H.** MMP16 expression was detected by qRT-PCR and Western blotting analysis in HCC tissues and the matched normal liver tissues. **G.** The linear correlation of miR-139-5p and MMP16 was determined by Spearman correlation analysis in HCC tissues. **I.** MMP16 protein expression was detected by Western blotting analysis in THLE-2, Hep3B and Huh-7 cells. ***P*<0.01, ****P*<0.001 and *****P*<0.0001.

after MMP16 overexpression. Subsequently, MMP16 introduction relieved the inhibitory effects of Matrine on cell viability and proliferation and the promoting effect on cell apoptosis (Fig. 6B-D). The invasion and tube formation of Hep3B and Huh-7 cells were also inhibited by Matrine; however, these effects were rescued when MMP16 expression was increased (Fig. 6E,F). Further, ectopic MMP16 expression antagonized the repressive effects of Matrine on the protein expression of CyclinD1 and N-cadherin (Fig. 6G,H). Collectively, these data manifested that Matrine was able to inhibit HCC cell processes through MMP16.

Circ_0013290 depletion inhibited HCC cell malignancy by regulating MMP16

Based on the above results, we analyzed whether MMP16 was involved in the regulation of circ_0013290 toward HCC cell malignancy. To this end, the small hairpin RNA of circ_0013290 and the overexpression plasmid of MMP16 were co-transfected into HCC cells (Hep3B and Huh-7 cells). The data of Fig. 7A confirmed the success of circ_0013290 knockdown in Hep3B and Huh-7 cells. Subsequently, circ_0013290 depletion significantly reduced MMP16 protein expression, whereas the effect was attenuated after MMP16 introduction (Fig. 7B). Circ_0013290 absence inhibited cell viability and proliferation but induced cell apoptosis, but these effects were rescued when MMP16 expression was increased (Fig. 7C-E). Consistently, the inhibitory effects of circ_0013290 silencing on the invasion and tube formation of Hep3B and Huh-7 cells were overturned by increasing MMP16 expression (Fig. 7F,G). Further, circ_0013290-reduced expression of CyclinD1 and N-cadherin was restored after MMP16 introduction (Fig. 7H,I). Taken together, these data demonstrated circ_0013290 modulated HCC cell malignancy through MMP16.

Circ_0013290 modulated MMP16 expression through miR-139-5p in HCC cells

We silenced circ_0013290 and miR-139-5p in Hep3B and Huh-7 cells and then analyzed the consequential effects on MMP16 protein expression. As shown in Figure 8A,B, circ_0013290 silencing significantly reduced MMP16 protein expression, whereas the effect was weakened when miR-139-5p

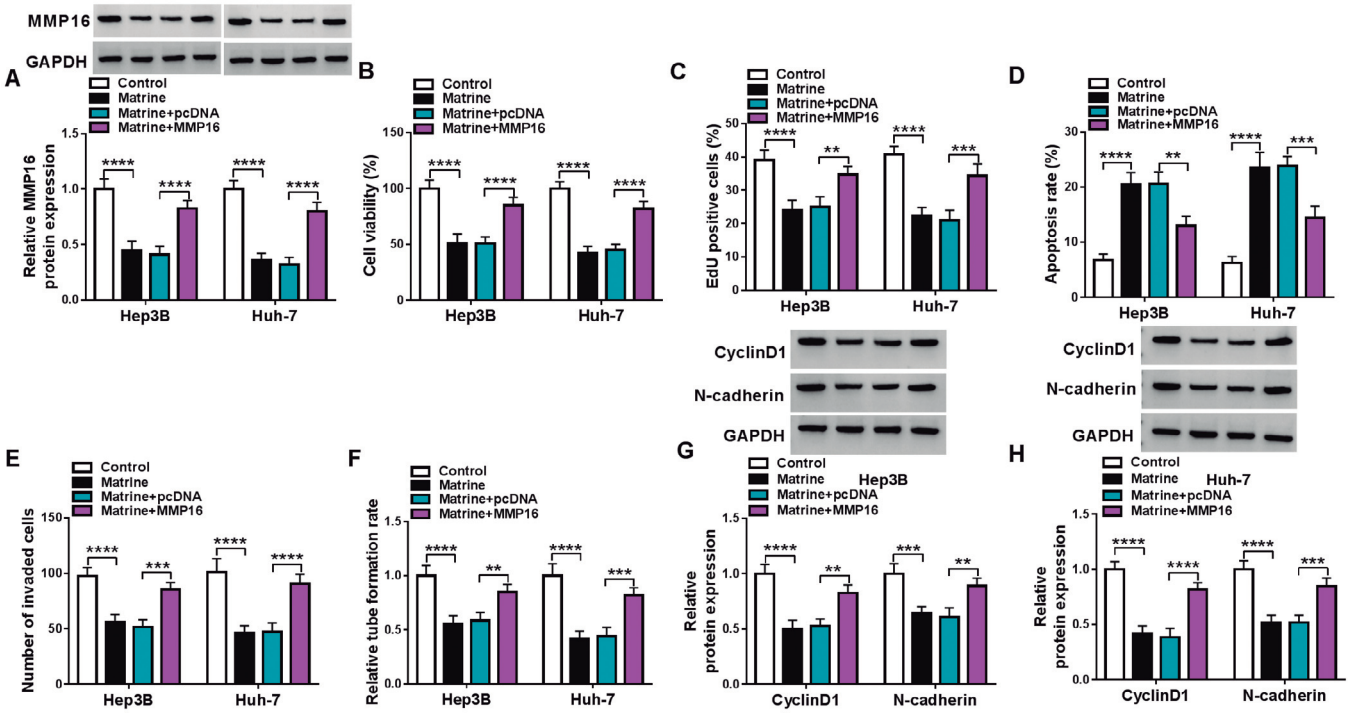

Fig. 6. Matrine inhibited HCC cell processes through MMP16. **A-H.** Hep3B and Huh-7 cells were treated with Matrine, Matrine+pcDNA or Matrine+MMP16, and untreated Hep3B and Huh-7 cells were employed as controls. **A.** MMP16 protein expression was detected by Western blotting analysis. **B.** Cell viability was analyzed by CCK-8 assay. **C.** Cell proliferation was evaluated by EdU assay. **D.** Flow cytometry analysis was performed to assess cell apoptosis. **E.** Transwell invasion assay was conducted to analyze cell invasion. **F.** The tube formation of Hep3B and Huh-7 cells was investigated by tube formation assay. **G, H.** The protein expression of CyclinD1 and N-cadherin was checked by Western blotting analysis. ***P*<0.01, ****P*<0.001 and *****P*<0.0001.

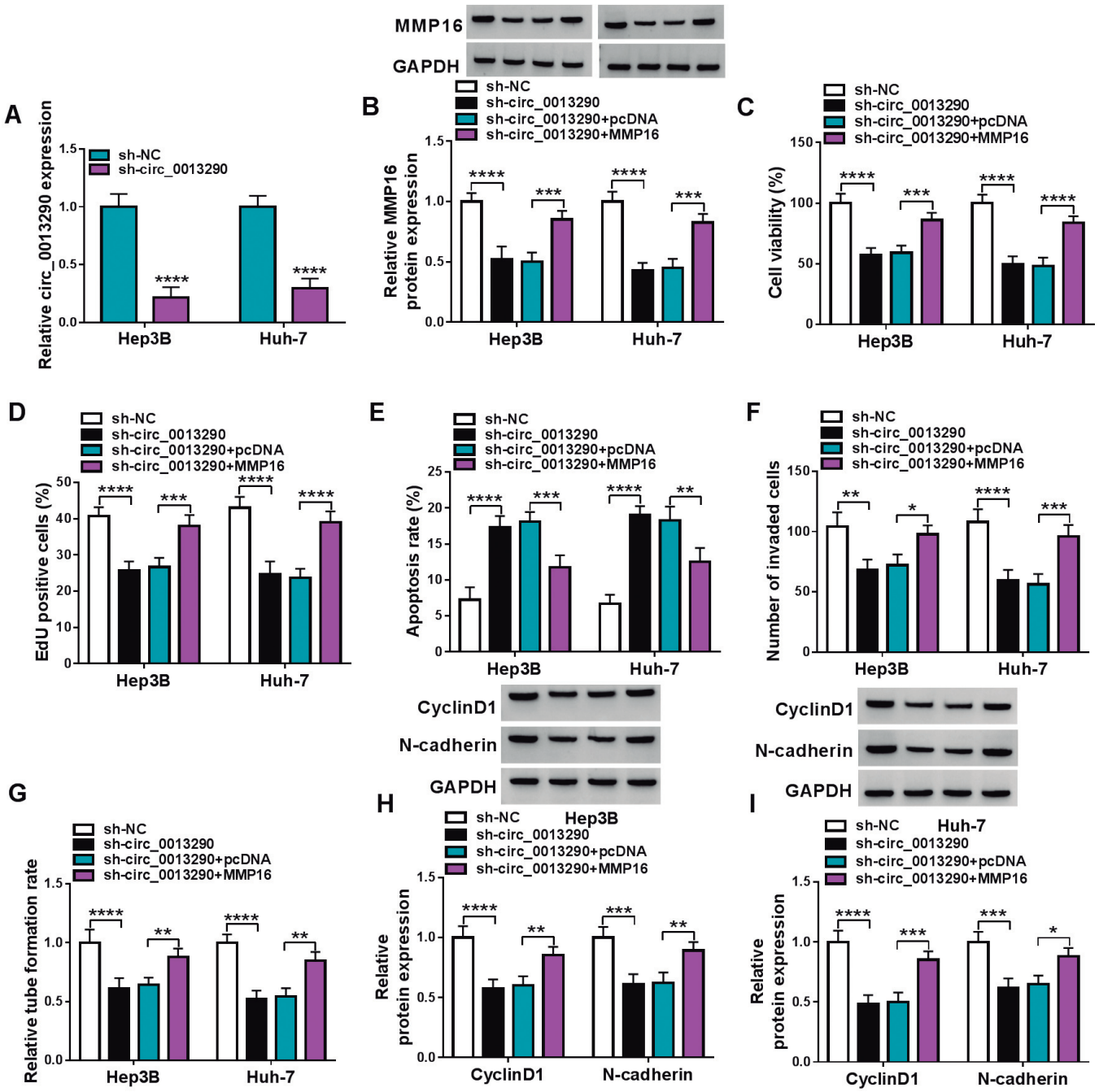

Fig. 7. Circ_0013290 modulated HCC cell malignancy through MMP16. **A.** The expression of circ_0013290 was detected by qRT-PCR in Hep3B and Huh-7 cells transfected with sh-circ_0013290 or sh-NC. **B-I.** Hep3B and Huh-7 cells were transfected with sh-NC, sh-circ_0013290, sh-circ_0013290+pcDNA or sh-circ_0013290+MMP16, and MMP16 protein expression was analyzed by Western blotting analysis **(B)**, cell viability by CCK-8 assay **(C)**, cell proliferation by EdU assay **(D)**, cell apoptosis by flow cytometry analysis **(E)**, cell invasion by transwell invasion assay **(F)**, angiogenic capacity by tube formation assay **(G)**, and the protein expression of CyclinD1 and N-cadherin by Western blotting analysis **(H, I)**. **P*<0.05, ***P*<0.01, ****P*<0.001 and *****P*<0.0001.

expression was decreased, implying that circ_0013290 can control MMP16 expression by interacting with miR-139-5p.

Circ_0013290 depletion enhanced Matrine-induced inhibition of tumor tumorigenesis in vivo

Given that *in vitro* data demonstrated that circ_0013290 overexpression counteracted Matrine-mediated HCC cell malignancy, we further evaluated whether circ_0013290 depletion improved the effect of Matrine on tumor formation *in vivo*. To verify this, we conducted a xenograft mouse model assay. As shown in Figure 9A,B, the mice treated with sh-NC+Matrine had smaller tumor and weight, and those treated with sh-circ_0013290+Matrine had the smaller tumor and weight than controls. Moreover, the combination treatment led to the lowest levels of circ_0013290 and MMP16 expression, and the highest level of miR-139-5p expression in the forming tumors (Fig. 9C-E). In accordance, the combination treatment group showed the lowest expression of MMP16, CyclinD1 and N-cadherin in the primary tumors from Huh-7 cells, as revealed by IHC assay (Fig. 9F). These data demonstrated that Matrine inhibited tumor tumorigenesis by regulating circ_0013290 expression.

Discussion

Natural plant extracts that exert antitumor activity by inhibiting cancer cell proliferation, increasing cell apoptosis, hindering cell metastasis and reducing the toxicity of anticancer agents have emerged as promising anticancer agents. Matrine is an alkaloid that has been confirmed to have therapeutic benefits for cancers (Zhang et al., 2020a). This study investigated the role of the alkaloid in HCC progression and the related mechanism. Our evidence suggested that Matrine inhibited HCC cell malignancy through the circ_0013290/miR-139-5p/MMP16 pathway.

Accumulating evidence has suggested that Matrine exhibits antitumor activity in different cancers. For example, Matrine inhibited breast cancer development by inducing cell apoptosis as well as autophagy through the AKT/mTOR pathway (Du et al. 2020b). As analyzed by Liu et al. Matrine inhibited the function of PC cells by regulating the miR-93-5p/AHNAK nucleoprotein pathway (Liu et al., 2020). In addition, previous studies have indicated that Matrine inhibited HCC cell proliferation, apoptosis, autophagy, motility or cell stemness by regulating circRNA (Lin et al., 2020), inhibiting the β-catenin signaling pathway (Dai et al., 2019), and suppressing epithelial-mesenchymal transition (Wang et al., 2018). Another study also suggested that the Matrine derivative WM622 ($C_{26}H_{35}ON_3S_2$) could inhibit HCC cell growth and induce apoptosis via inactivating the PI3K/AKT signal pathway (Sun et al., 2018). Our study indicated that Matrine inhibited HCC cell proliferation and invasion, and induced apoptosis. Besides, the work provided evidence that Matrine inhibited tube formation of HCC cells.

CircRNA is a product of backsplicing on precursor mRNA, and increasing studies expound that circRNA plays key parts in HCC (Han et al., 2020). The underlying mechanism of Matrine regulating cancer progression is also associated with circRNA (Lin et al., 2020). The study subsequently proved that circ_0013290

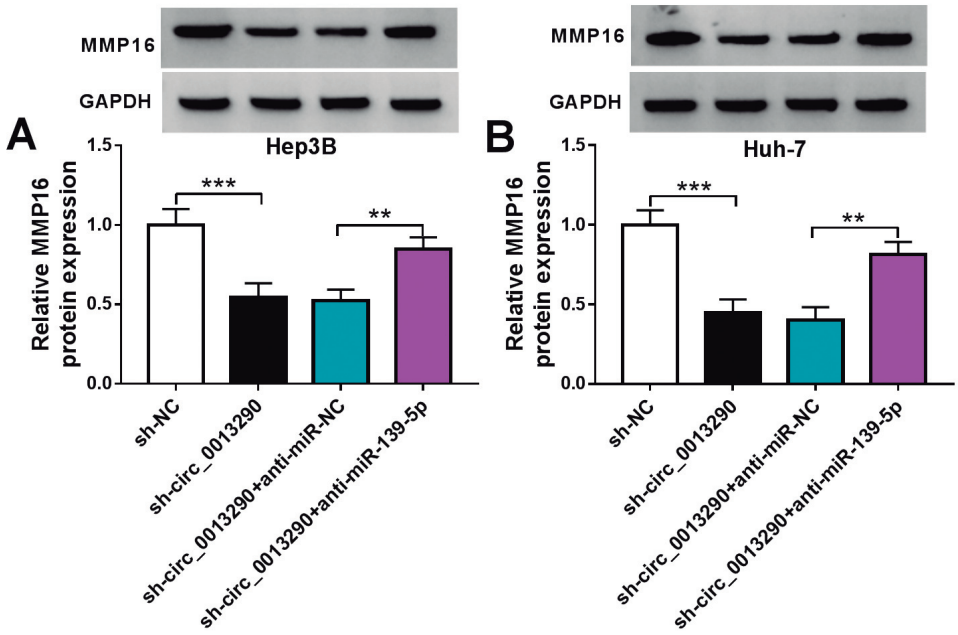

Fig. 8. Circ_0013290 modulated MMP16 expression through miR-139-5p in HCC cells. Both Hep3B and Huh-7 cells were transfected with sh-NC, sh-circ_0013290, sh-circ_0013290+anti-miR-NC or sh-circ_0013290+anti-miR-139-5p, and MMP16 protein expression was analyzed by Western blotting analysis **(A, B)**. $^{**}P<0.01$ and $^{***}P<0.001$.

was involved in the anticancer effects of Matrine against HCC. Here, we found the high expression of circ_0013290 in HCC tissues and cells. CircRNA is resistant to exonuclease due to its lack of a 5' or 3' polarities structure (Memczak et al., 2013). Thus, we analyzed circ_0013290 stability using RNase R. As expected, circ_0013290 was resistant to RNase R activity. Importantly, we found that the regulation of Matrine toward HCC cell processes involved the downregulation of circ_0013290.

Considering the miRNA sponge effect of circRNA (Panda, 2018), we analyzed the circ_0013290-associated miRNA in HCC cells. MiR-139-5p was downregulated in HCC, and its overexpression inhibited HCC cell invasion and induced cell apoptosis (Li et al., 2019). MiR-139-5p combined with SLIT and NTRK like family member4 (SLITRK4) to regulate HCC cell proliferation and invasion (Wu et al., 2020). In addition, miR-139-5p inhibited the epithelial-mesenchymal transition of HCC cells by binding to Wilms' tumor 1-associating protein (Liu et al., 2021). But the association of circ_0013290 with miR-139-5p in HCC has not been reported. Thus, we focused on the miRNA in subsequent studies. In accordance, the study found the downregulation of miR-139-5p in HCC tissues and cells. Based on the above evidence, we hypothesized that miR-139-5p participated in Matrine-induced effects in HCC cells. As analyzed by rescue assays, miR-139-5p inhibitors relieved the inhibitory effects of Matrine on HCC cell processes, proving our hypothesis. Meanwhile, *in vivo* data showed that circ_0013290 depletion-increased miR-139-5p expression was enhanced by Matrine. The above data suggested that miR-139-5p was involved in the mechanism of Matrine regulating HCC progression.

Chronic inflammation can remodel extracellular matrix (ECM) to promote human cancer progression (Stark et al., 2015). Alternation in ECM integrity is correlated with poorer prognosis for cancer patients (Socovich and Naha, 2019). The alterations toward both stiffness and degradation of ECM can promote tumor growth (Najafi et al., 2019), which requires attention in the area of therapy. Extracellular matrix transfer is important for cell invasion and metastasis, and MMPs have been expounded to regulate cell migration and invasion processes (Hadler-Olsen et al., 2013). With respect to the mechanism, MMPs degrade the extracellular matrix of tumors to lead to tumor development (Wörmann, 2017). The present study has suggested that Matrine can inhibit HCC malignancy by reducing HCC cell invasion. MMP16, a member of the

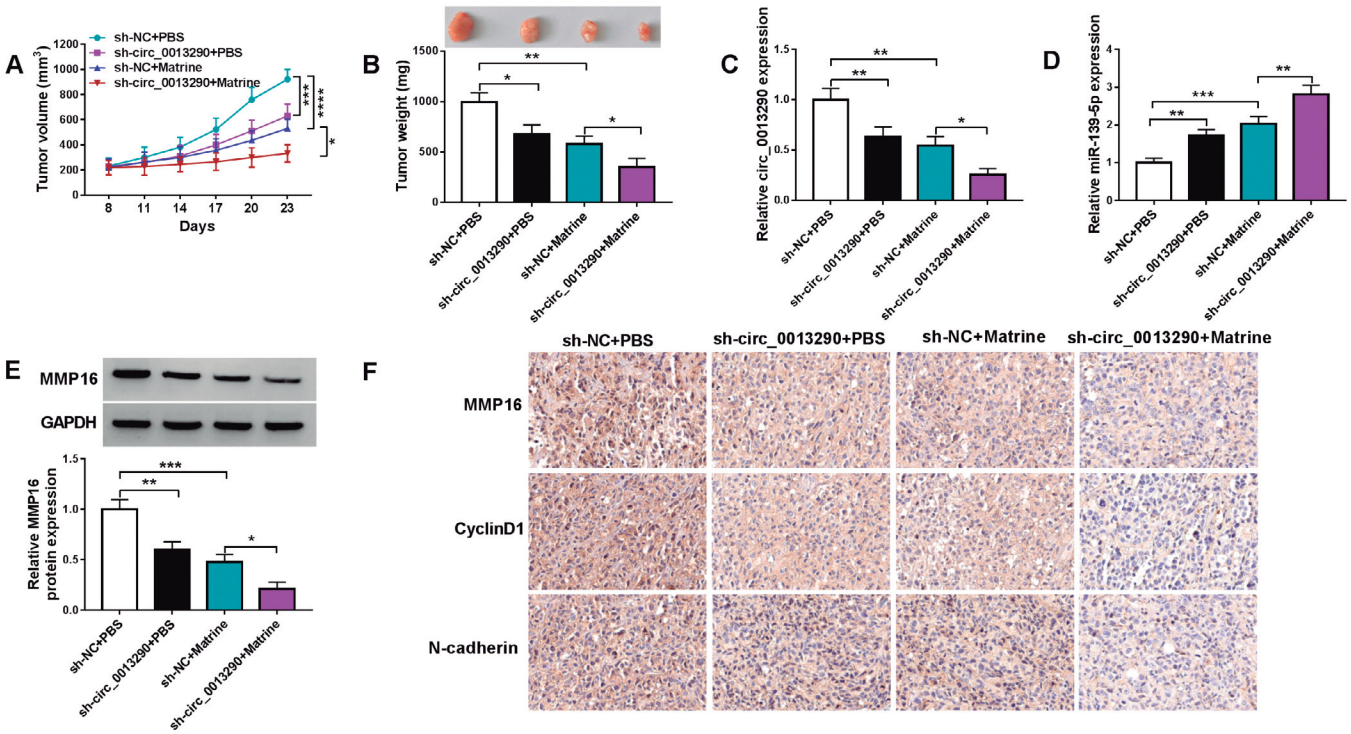

Fig. 9. Matrine inhibited tumor tumorigenesis by regulating circ_0013290 expression. Huh-7 cells treated with sh-NC+PBS, sh-circ_0013290+PBS, sh-NC+Matrine or sh-circ_0013290+Matrine were injected into nude mice, and the forming tumors were harvested on the 23rd day after injection. **A, B.** The volume and weight of the tumors were measured. **C-E.** Circ_0013290, miR-139-5p and MMP16 expression were analyzed by qRT-PCR or Western blotting analysis in the primary tumors from Huh-7 cells. **F.** IHC assay was conducted to assess the protein expression of MMP16, CyclinD1 and N-cadherin in the tumors. **P*<0.05, ***P*<0.01, ****P*<0.001 and *****P*<0.0001.

MMPs family, has been documented to promote HCC progression (Shen et al., 2017; Zhou and Chen, 2021). Herein, we hypothesized that the regulation of Matrine on HCC involved MMP16. As expected, we found that MMP16 overexpression relieved the effects of Matrine on HCC cell processes. Also, the increased expression of MMP16 remitted the impacts of circ_0013290 depletion on HCC cell malignancy. Based on the above results, we analyzed the relationship between miR-139-5p and MMP16. Our evidence suggested that miR-139-5p targeted MMP16. Consistently, circ_0013290 combined with miR-139-5p to induce MMP16 production. *In vivo* data demonstrated that Matrine enhanced circ_0013290 depletion-reduced MMP16 expression. Therefore, we concluded that Matrine inhibited HCC progression through the circ_0013290/miR-139-5p/MMP16 pathway.

In summary, this study disclosed the anticancer effects of Matrine against HCC. In terms of mechanism, the inhibitory effects of Matrine on HCC development were attributed to the decreased expression of circ_0013290 and the subsequent impact on the miR-139-5p/MMP16 pathway. The finding suggests that Matrine has the potential as an anti-HCC medication.

Acknowledgements. None.
Disclosure of interest. The authors declare that they have no conflicts of interest.
Funding. None.

References

Chi G., Xu D., Zhang B. and Yang F. (2019). Matrine induces apoptosis and autophagy of glioma cell line U251 by regulation of circRNA-104075/BCL-9. Chem. Biol. Interact. 308, 198-205.

Cho Y.R., Lee J.H., Kim J.H., Lee S.Y., Yoo S., Jung M.K., Kim S.J., Yoo H.J., Pack C.G., Rho J.K. and Son J. (2018). Matrine suppresses KRAS-driven pancreatic cancer growth by inhibiting autophagy-mediated energy metabolism. Mol. Oncol. 12, 1203-1215.

Dai M., Cai Z., Chen N., Li J., Wen J., Tan L. and Guo D. (2019). Matrine suppresses stemness of hepatocellular carcinoma cells by regulating β-catenin signaling pathway. Nan Fang Yi Ke Da Xue Xue Bao. 39, 1239-1245 (in chinese).

Draper A. (2020). A concise review of the changing landscape of hepatocellular carcinoma. Am. J. Manag. Care 26, S211-s219.

Du F., Cao T., Xie H., Li T., Sun L., Liu H., Guo H., Wang X., Liu Q., Kim T., Franklin J.L., Graves-Deal R., Han W., Tian Z., Ge M., Nie Y., Fan D., Coffey R.J., Lu Y. and Zhao X. (2020a). KRAS mutation-responsive mir-139-5p inhibits colorectal cancer progression and is repressed by Wnt signaling. Theranostics 10, 7335-7350.

Du J., Li J., Song D., Li Q., Li L., Li B. and Li L. (2020b). Matrine exerts anti-breast cancer activity by mediating apoptosis and protective autophagy via the AKT/mTOR pathway in MCF-7 cells. Mol. Med. Rep. 22, 3659-3666.

Hadler-Olsen E., Winberg J.O. and Uhlin-Hansen L. (2013). Matrix metalloproteinases in cancer: their value as diagnostic and prognostic markers and therapeutic targets. Tumour Biol. 34, 2041-2051.

Han T.-S., Hur K., Cho H.-S. and Ban H.S. (2020). Epigenetic Associations between lncRNA/circRNA and miRNA in Hepatocellular Carcinoma. Cancers 12, 2622.

He Z., Ruan X., Liu X., Zheng J., Liu Y., Liu L., Ma J., Shao L., Wang D., Shen S., Yang C. and Xue Y. (2019). FUS/circ_002136/miR-138-5p/SOX13 feedback loop regulates angiogenesis in glioma. J. Exp. Clin. Cancer Res. 38, 65-65.

Hua S., Lei L., Deng L., Weng X., Liu C., Qi X., Wang S., Zhang D., Zou X., Cao C., Liu L. and Wu D. (2018). miR-139-5p inhibits aerobic glycolysis, cell proliferation, migration, and invasion in hepatocellular carcinoma via a reciprocal regulatory interaction with ETS1. Oncogene 37, 1624-1636.

Huang D.-W., Huang M., Lin X.-S. and Huang Q. (2017). CD155 expression and its correlation with clinicopathologic characteristics, angiogenesis, and prognosis in human cholangiocarcinoma. Onco Targets Ther. 10, 3817-3825.

Huang H., Wang Q., Du T., Lin C., Lai Y., Zhu D., Wu W., Ma X., Bai S., Li Z., Liu L. and Li Q. (2018). Matrine inhibits the progression of prostate cancer by promoting expression of GADD45B. Prostate 78, 327-335.

Intaraprasong P., Siramolpiwat S. and Vilaichone R.K. (2016). Advances in management of hepatocellular carcinoma. Asian Pac. J. Cancer Prev. 17, 3697-3703.

Kulcheski F.R., Christoff A.P. and Margis R. (2016). Circular RNAs are miRNA sponges and can be used as a new class of biomarker. J. Biotechnol. 238, 42-51.

Li J., He X., Wu X., Liu X., Huang Y. and Gong Y. (2020). miR-139-5p inhibits lung adenocarcinoma cell proliferation, migration, and invasion by targeting MAD2L1. Comput. Math. Methods Med. 2020, 2953598.

Li P., Xiao Z., Luo J., Zhang Y. and Lin L. (2019). MiR-139-5p, miR-940 and miR-193a-5p inhibit the growth of hepatocellular carcinoma by targeting SPOCK1. J. Cell Mol. Med. 23, 2475-2488.

Lin S., Zhuang J., Zhu L. and Jiang Z. (2020). Matrine inhibits cell growth, migration, invasion and promotes autophagy in hepatocellular carcinoma by regulation of circ_0027345/miR-345-5p/HOXD3 axis. Cancer Cell Int. 20, 246.

Liu W., Gao X., Chen X., Zhao N., Sun Y., Zou Y., Guan Y., Yang L., Pei X., Wang G., Wang B., Li M. and Song W. (2021). miR-139-5p loss-mediated WTAP activation contributes to hepatocellular carcinoma progression by promoting the epithelial to mesenchymal transition. Front. Oncol. 11, 611544.

Liu Z.M., Yang X.L., Jiang F., Pan Y.C. and Zhang L. (2020). Matrine involves in the progression of gastric cancer through inhibiting miR-93-5p and upregulating the expression of target gene AHNAK. J. Cell Biochem. 121, 2467-2477.

Luo X., Liu Y., Li H., Cheng T., Wu J., Chen L., Ju L., Cai W. and Bian Z. (2021). Hsa_circ_0013290 acts as cancer-promoting gene in hepatocellular carcinoma. Cancer Control 28, 10732748211055681.

Memczak S., Jens M., Elefsinioti A., Torti F., Krueger J., Rybak A., Maier L., Mackowiak S.D., Gregersen L.H., Munschauer M., Loewer A., Ziebold U., Landthaler M., Kocks C., le Noble F. and Rajewsky N. (2013). Circular RNAs are a large class of animal RNAs with regulatory potency. Nature 495, 333-338.

Najafi M., Farhood B. and Mortezaee K. (2019). Extracellular matrix (ECM) stiffness and degradation as cancer drivers. J. Cell Biochem. 120, 2782-2790.

Paganoni R., Lechel A. and Vujic Spasic M. (2021). Iron at the interface

of hepatocellular carcinoma. Int. J. Mol. Sci. 22, 4097.

Panda A.C. (2018). Circular RNAs act as miRNA sponges. Adv. Exp. Med. Biol. 1087, 67-79.

Qu S., Yang X., Li X., Wang J., Gao Y., Shang R., Sun W., Dou K. and Li H. (2015). Circular RNA: A new star of noncoding RNAs. Cancer Lett. 365, 141-148.

Rashid H.U., Xu Y., Muhammad Y., Wang L. and Jiang J. (2019). Research advances on anticancer activities of matrine and its derivatives: An updated overview. Eur. J. Med. Chem. 161, 205-238.

Salmena L., Poliseno L., Tay Y., Kats L. and Pandolfi P.P. (2011). A ceRNA hypothesis: the Rosetta Stone of a hidden RNA language? Cell 146, 353-358.

Shen Z., Wang X., Yu X., Zhang Y. and Qin L. (2017). MMP16 promotes tumor metastasis and indicates poor prognosis in hepatocellular carcinoma. Oncotarget 8, 72197-72204.

Socovich A.M. and Naba A. (2019). The cancer matrisome: From comprehensive characterization to biomarker discovery. Semin. Cell Dev. Biol. 89, 157-166.

Sohal D.P. and Sun W. (2011). Hepatocellular carcinoma: prevention and therapy. Curr. Oncol. Rep. 13, 186-194.

Stark T., Livas L. and Kyprianou N. (2015). Inflammation in prostate cancer progression and therapeutic targeting. Transl. Androl. Urol. 4, 455-463.

Sun X., Zhuo X.B., Hu Y.P., Zheng X. and Zhao Q.J. (2018). A novel matrine derivative WM622 inhibits hepatocellular carcinoma by inhibiting PI3K/AKT signaling pathways. Mol. Cell Biochem. 449, 47-54.

Sung H., Ferlay J., Siegel R.L., Laversanne M., Soerjomataram I., Jemal A. and Bray F. (2021). Global Cancer Statistics 2020: GLOBOCAN estimates of incidence and mortality worldwide for 36 cancers in 185 countries. CA Cancer J. Clin. 71, 209-249.

Wang Y., Zhang S., Liu J., Fang B., Yao J. and Cheng B. (2018). Matrine inhibits the invasive and migratory properties of human hepatocellular carcinoma by regulating epithelial-mesenchymal transition. Mol. Med. Rep. 18, 911-919.

Wei Y.P., Wang X.H., Liu G., Zhang J.F., Yang Y.X., Zhang J., Song X.L., Li Z.D. and Zhao L.D. (2018). Matrine exerts inhibitory effects in melanoma through the regulation of miR-19b-3p/PTEN. Int. J. Oncol. 53, 791-800.

Wörmann B. (2017). Breast cancer: basics, screening, diagnostics and treatment. Med. Monatsschr. Pharm. 40, 55-64.

Wu J., Zhang T., Chen Y. and Ha S. (2020). MiR-139-5p influences hepatocellular carcinoma cell invasion and proliferation capacities via decreasing SLITRK4 expression. Biosci. Rep. 40, BSR20193295.

Xu P., Wang L., Xie X., Hu F., Yang Q., Hu R., Jiang L., Ding F., Mei J., Liu J. and Xiao H. (2020). Hsa_circ_0001869 promotes NSCLC progression via sponging miR-638 and enhancing FOSL2 expression. Aging (Albany NY) 12, 23836-23848

Zhang X., Hou G., Liu A., Xu H., Guan Y., Wu Y., Deng J. and Cao X. (2019). Matrine inhibits the development and progression of ovarian cancer by repressing cancer associated phosphorylation signaling pathways. Cell Death Dis. 10, 770.

Zhang H., Chen L., Sun X., Yang Q., Wan L. and Guo C. (2020a). Matrine: A promising natural product with various pharmacological activities. Front. Pharmacol. 11, 588-588.

Zhang H., Shen Y., Li Z., Ruan Y., Li T., Xiao B. and Sun W. (2020b). The biogenesis and biological functions of circular RNAs and their molecular diagnostic values in cancers. J. Clin. Lab. Anal. 34, e23049.

Zhou H. and Chen Y. (2021). CircRNA has_circ_0001806 promotes hepatocellular carcinoma progression via the miR-193a-5p/MMP16 pathway. Braz. J. Med. Biol. Res. 54, e11459.

Zhou W., Wang J., Qi Q., Feng Z., Huang B., Chen A., Zhang D., Li W., Zhang Q., Bjerkvig R., Li X. and Wang J. (2018). Matrine induces senescence of human glioblastoma cells through suppression of the IGF1/PI3K/AKT/p27 signaling pathway. Cancer Med. 7, 4729-4743.

Zhu L., Pan Q.X., Zhang X.J., Xu Y.M., Chu Y.J., Liu N., Lv P., Zhang G.X. and Kan Q.C. (2016). Protective effects of matrine on experimental autoimmune encephalomyelitis via regulation of ProNGF and NGF signaling. Exp. Mol. Pathol. 100, 337-343.

Accepted December 14, 2022